Massive multiplication of genome and ribosomes in dormant cells (akinetes) of *Aphanizomenon ovalisporum* (Cyanobacteria)

Assaf Sukenik[1], Ruth N. Kaplan-Levy[1] Jessica Mark Welch[2] and Anton F. Post[2]

1. The Yigal Allon Kinneret Limnological Laboratory, Israel Oceanographic & Limnological Research P.O.Box 447 Migdal 14950, Israel
2. The Josephine Bay Paul Center for Comparative Molecular Biology and Evolution, Marine Biology Laboratory, 7 MBL St, Woods Hole, MA 02543 USA

Corresponding author: Assaf Sukenik; The Yigal Allon Kinneret Limnological Laboratory, Israel Oceanographic & Limnological Research P.O.Box 447 Migdal 14950, Israel.
Tel: +972 4 6721444 ext 205
Fax: +972 4 6724627
e-mail: assaf@ocean.org.il

Running title: Genome and ribosome multiplication in akinetes

Key words: akinetes/ cyanobacteria/ dormancy/ fluorescence *in situ* hybridization/ polyphosphate/ polyploidy/ laser microdissection microscopy

Abstract

Akinetes are dormancy cells commonly found among filamentous cyanobacteria, many of which are toxic and/or nuisance, bloom-forming species. Development of akinetes from vegetative cells is a process that involves morphological and biochemical modifications. Here we applied a single cell approach to quantify genome and ribosome content of akinetes and vegetative cells in *Aphanizomenon ovalisporum* (Cyanobacteria). Vegetative cells of *A. ovalisporum* were naturally polyploid and contained on average 8 genome copies per cell. However, the chromosomal content of akinetes increased up to 450 copies, with an average value of 119 genome copies per akinete, 15 fold higher that in vegetative cells. Based on fluorescence *in situ* hybridization with a probe targeting 16S rRNA and detection with confocal laser scanning microscopy we conclude that ribosomes accumulated in akinetes to a higher level than that found in vegetative cells. We further present evidence that this massive accumulation of nucleic acids in akinetes is likely supported by phosphate supplied from inorganic polyphosphate bodies that were abundantly present in vegetative cells, but notably absent from akinetes. These results are interpreted in the context of cellular investments for proliferation following long term dormancy, as the high nucleic acid content would provide the basis for extended survival, rapid resumption of metabolic activity and cell division upon germination.

Introduction

Members of the order Nostocales are abundant, bloom-forming cyanobacteria. They are found in diverse aquatic environments such as fresh water lakes and reservoirs, estuaries, coastal lagoons, and the open ocean. Major blooms have been reported in Australia, Northern Europe, India, New Zealand, South Africa, USA and the Baltic Sea (Carmichael et al 1990, Codd 1999, Hudnell et al 2008), indicating a phenomenon of global dimensions. Many Nostocales species produce potent toxins that have been associated with livestock deaths, water quality deterioration and seafood contamination (van Apeldoorn et al 2007, Codd et al 2005, Dittmann and Wiegand 2006). The ability to develop akinetes (spore-like cells) is a survival trait of the Nostocales that provides these toxic species with a competitive advantage over other phytoplankton. Akinetes differentiate from vegetative cells and provide a seed bank for rapid repopulation of the water column (Hori et al 2003, Karlsson-Elfgren et al 2004). These dormant cells survive harsh conditions in bottom sediments and dried-up shores of streams, pools and lakes. As conditions improve, akinetes germinate and the resulting vegetative cells disperse, aided by newly formed gas vacuoles (Kaplan-Levy et al 2010, Hense and Beckmann 2010). Morphologically, akinetes are larger and have a thicker cell wall than do vegetative cells. They contain storage compounds (i.e. cyanophycin, glycogen) and a large amount of nucleic acid. Akinetes of *Anabaena cylindrica* contained twice as much DNA and 10-fold more protein than vegetative cells (Simon 1977). These high values are in part the consequence of the increased cell size of akinetes, up to ten times the volume of the vegetative cells (Fay 1969a, Fay 1969b). DAPI staining of *Aphanizomenon ovalisporum* akinetes demonstrated the accumulation of nucleic acids, their homogeneous dispersion over the entire akinete volume and the conspicuous absence of inorganic polyphosphate (IPP) bodies (Sukenik et al 2009). Here we applied a single cell approach to delineate the DAPI signal and demonstrate both a dramatic accumulation of genome copies and an enlarged ribosome pool in mature akinetes. These changes are interpreted in the context of cellular differentiation and modification toward long term dormancy, survival and rapid resumption of cell division upon germination.

Materials & Methods

Culture maintenance and growth

Stock and experimental cultures of *Aphanizomenon ovalisporum* (strain ILC-164 from Lake Kinneret, Israel; Banker et al 1997) were grown in liquid batch culture and transferred bi-weekly into freshly prepared BG11 medium in a 10-fold dilution (Stanier et al 1971). Cultures were grown in 100-250 ml flat tissue-culture flasks at 24±1 ºC on an orbital shaker with continuous agitation at

100 rpm and continuous illumination at 30 μmol quanta·m^{-2}·s^{-1}. For the induction of akinete development, trichomes from 6-day-old exponential cultures were harvested by centrifugation (3000 rcf), washed with, and transferred into akinete-inducing medium (BG11 medium depleted of K^+ ions, as previously described; Sukenik et al 2007). Differentiation of cells into akinetes was recognized by visual inspection under a Zeiss dissecting microscope (40X magnification) and defined based on cellular dimensions (akinetes have larger diameter) and shape as previously described (Sukenik et al 2007, Sukenik et al 2009).

Laser microdissection microscopy

Laser microdissection and laser pulse catapulting (LMPC) of vegetative cells and akinetes was performed with a PALM Combisystem that included an Axiovert 200 M microscope interfaced with RoboMover controlled by RoboSoftware v2.0 (Carl Zeiss MicroImaging GmbH, Germany). This is a fully automated, contamination-free, non-contact technology for sample capturing and collection by laser-induced transport. Using a laser pulse, a selected specimen is transported out of the object plane into a collection device such a lid of a microfuge tube. *A. ovalisporum* samples were air-dried on 0.17 mm microscope slides (50X25 mm), inspected and selected based on pigment fluorescence using a Zeiss fluorescence filter block (TRITC: BP535/50x; DCXRU 585; LP590m) or bright field image (halogen transmitted light using DIC condenser and 100X objective (Zeiss Fluar 100X /1.3 N.A.). Akinetes or vegetative cells were individually selected, laser excised and catapulted into the lid of a 200 μl adhesive-cap tube (Carl Zeiss #415190-9191-000) or into a wet lid of a standard 200 μl PCR tube. Predetermined numbers (1-5) of free akinetes were collected per tube. Similarly, filament-attached akinetes or vegetative cells from exponentially grown and akinete-induced cultures were collected. Spots of air-dried filtrate of culture suspensions were dissected, catapulted to collection tubes and used as negative controls.

DNA extraction and qPCR protocols

Quantitative PCR of LMPC collected samples was performed either directly or following DNA extraction using a QIAamp DNA Mini Kit (Qiagen). For this purpose, cell cohorts collected in adhesive-cap tubes were resuspended in a sterile water-buffer solution and DNA was extracted according to the manufacturer's protocol. Alternatively, laser-disrupted cells in the collecting tube lid were directly resuspended in the 1X PCR mix (SYBR Green PCR Master Mix, Applied Biosystems, USA) amended with the appropriate primers (Table 1). Samples were quickly centrifuged and copy numbers of the target gene (*16S rRNA* or *ntcA*) in the DNA template were

quantified using the StepOnePlus™ Real-Time PCR System Applied Biosystems, USA). Real-time PCR assays were performed in a final volume of 20 µL using SYBR Green PCR Master Mix (Applied Biosystems, USA). All reactions were performed with a StepOnePlus™ Real-Time PCR System using the following cycling protocol: 95 °C for 30 s followed by 45 cycles at 95 °C for 5 s and 60 °C for 30 s. At the end of each run, a DNA dissociation analysis (melting curve) was performed to ensure the absence of primer-dimers, mixed amplicon populations and/or nonspecific products. A single direct PCR assay was performed for each sample collected by the laser dissection protocol. Triplicates of the same sample were performed only when DNA extraction was carried out prior to the qPCR step. Due to low DNA content most analyses consumed the entire sample and replication was obtained on large numbers of cells collected from the same culture. We targeted *16S rRNA* and the nitrogen regulatory gene *ntcA* to determine gene (and thus genome) copy numbers. Four copies of the *16S rRNA* gene were identified along the *A. ovalisporum* genome. They occurred as two identical pairs that differed by a single nucleotide (GenBank accession JF768742 to JF768745). The *ntcA* gene was recognized as a single copy. Whereas both target genes should in theory yield identical genome copy numbers, it is clear that the higher copy number of 16S rRNA enhances detection and resolution of qPCR with single cell templates. A standard curve and a no-template control were included in each qPCR run. Standard curves were constructed using different concentrations of a plasmid that contained a fragment of the target gene (*16S rRNA* or *ntcA*) of *A. ovalisporum*. The concentration of the cloned plasmid stock solution was measured using a Nanodrop 2000 spectrophotometer (Thermo Scientific) and diluted to provide a series of different plasmid DNA concentrations.

Fluorescence in situ hybridization (FISH)

Exponentially growing and akinete-induced (10 days old) cultures of *A. ovalisporum* were washed in Phosphate Buffered Saline (PBS: 130 mM NaCl, 10 mM sodium phosphate buffer pH 8.4) and fixed in PBS containing 4% paraformaldehyde at 4 ºC for 2 hrs. The cells were then washed twice in PBS and collected by rapid centrifugation. The pellet was then resuspended in cold 100% methanol and incubated at 4 ºC for an additional 2 hrs. The fixed cells were collected by brief centrifugation, washed in lysozyme buffer (100 mM Tris-HCl pH 7.5 and 5 mM $MgCl_2$) and finally incubated with 1mg/mL lysozyme (Sigma L7651) at 37°C for 60 min. Lysozyme reactions were stopped by washing the sample several times in Tris-EDTA buffer (100 mM Tris-HCl pH 7.5 and 10 mM EDTA), followed by a short wash in hybridization buffer (900 mM NaCl, 20 mM Tris-HCl pH 7.5, 15 % (v/v) formamide). The cells were then re-suspended in 50 □l of hybr

The oligonucleotide probe EUB338 (Amann et al. 1990) labeled at the 5' end with Alexa 488

(Invitrogen Corp.) was added to final concentration of 1.4 µg/ml and samples were incubated overnight at 46ºC. For control experiments, samples were exposed to hybridization buffer that did not contain any probe. Cells were washed in washing buffer (900 mM NaCl, 20 mM Tris-HCl pH 7.5) and applied to microscope slides (Ultrastick, Gold Seal products Cat No 3039). Cells retained on the slide were washed in cold deionized water followed by 100% cold ethanol washes. The slides were air-dried; the sample was mounted in ProLong Gold anti-fade solution (Invitrogen), covered with a cover slip, cured overnight and kept in the dark until inspection by confocal microscopy.

Hoechst staining

Visualization of cellular DNA was facilitated by staining *A. ovalisporum* trichomes and akinetes with Hoechst 33258. Cultures (exponentially grown cultures and 10 day old akinete-induced cultures) were fixed in 4% paraformaldehyde and then in cold methanol as described above. The fixed cells were washed in PBS, resuspended in 50 µl PBS containing 10 µg/mL Hoechst 33258 and incubated at room temperature for 2 hrs before the staining buffer was removed by centrifugation and repeated washes. Cells were applied to microscope slides as described above and kept dark until inspection by confocal microscopy.

Laser scanning confocal microscopy

A Zeiss LSM 710 confocal laser scanning microscope (Carl Zeiss MicroImaging GmbH, Germany) was used for spectral analysis of *A. ovalisporum* filaments and akinetes following their staining with fluorescent dyes. For FISH analyses, samples were excited with the 488 nm line of a 25 mW Ar laser, always using identical settings of laser power (0.5%) and other operational parameters to confirm that maximal emission fluorescence never exceeded the saturation value of the detector, and to provide the basis for comparative data analyses between samples from different treatments and within the same frame. Emission spectra between 496 and nm were recorded using the lambda scan function of the 'ZEN Software' (Carl Zeiss MicroImaging GmbH, Germany) by acquiring an array of 24 images each representing 9.6 nm of spectral width. Images of 1024X1024 pixels were collected using a Plan-Apochromat 20x/0.8 numerical aperture objective. Scans were performed at a line scan speed of 200 Hz (pixel dwell time 1.27 microseconds with averaging of 4 lines), and the confocal pinhole was opened to 173 µm diameter to image an 8.8 micron optical section. Samples stained with Hoechst 33258 were excited with the 405 nm laser line of a 30 mW diode 405-30, always using the same laser power settings (4 %) and other operational parameters.

Emission spectra between 429 and 716 nm were recorded by acquiring an array of 30 images at 9.6 nm intervals. Images of 512x512 pixels were collected at a line scan speed of 77 Hz (pixel dwell time 25.2 microseconds with no averaging) with the confocal pinhole opened to 118 μm diameter to image a 6 micron optical section. The Lambda Coded View of the ZEN Software supplied with the microscope was used to display a wavelength-coded color view (i.e. a color palette was automatically assigned to the individual images which are then displayed in a merge-type display). Mean fluorescence intensity was measured in regions of 5 pixels from a single vegetative cell or from a single akinete using the ZEN Software supplied with the microscope. The raw spectral data were corrected against a spectrum from control samples.

DAPI staining

The presence of nucleic acids and inorganic polyphosphate (Poly-P) bodies in vegetative cells and in developing akinetes was visualized by 4'-6-Diamidino-2-phenylindole (DAPI) staining, following the procedure proposed by Porter and Feig (1980). DAPI is known to form fluorescent complexes with natural double-stranded DNA but it also binds RNA (Kapuscinski 1995). DAPI also binds to inorganic Poly-P, resulting in a shift of the fluorescence emission to a longer wavelength with a maximum at about 525 nm (Siderius et al 1996). Subsamples of *Aphanizomenon* cultures were fixed with 0.6% formalin final concentration. Trichomes and free akinetes were collected on Nucleopore filters (0.2 μm pore size black polycarbonate membrane cat No. 11021 Poutris, USA) immersed in DAPI solution (0.6% in water) for 5 minutes, and gently washed with sterile water. Samples were observed in an epi-fluorescence microscope (Axioskop Zeiss, Germany) using a high pressure mercury source (HBO 200) interfaced with a Zeiss Filter set 02 (excitation G365, beam splitter FT 395 and emission LP 420).

Neisser staining

Confirmation of the presence of Inorganic Poly-P bodies in trichomes was based on Neisser staining (Bacteriologists 1957). Neisser negative cells (without Poly-P) are stained slightly brown or yellow, whereas Neisser positive cells with Poly-P bodies show dark purple-black colored globules.

Results

Accumulation of DNA in akinetes

Based on DAPI staining of akinetes and vegetative cells in induced cultures of *A. ovalisporum* we previously concluded that akinetes accumulate nucleic acids (Sukenik et al 2009). DAPI binds to DNA as well as to RNA, albeit at a lower fluorescence yield; therefore it provides little insight in the cellular processes underlying the nucleic acid accumulation. We applied a DNA-specific dye, Hoechst 33258, to study whether DNA replication continued during akinete differentiation and maturation, in the absence of cell division. High resolution spectral images were recorded by laser scanning confocal microscopy and presented as false-color images approximating the true colors using the "wavelength color-coded" setting (Figure 1). Vegetative cells showed a dominant red fluorescence signal that originated from excitation of photosynthetic pigments. Blue fluorescence derived from emission by Hoechst dye bound to DNA could hardly be visualized in vegetative cells due to high red fluorescence (Figure 1A), but was detected as relatively low 472 nm emission in the acquired spectral data (see Figure 2 and 3 below). Trichomes of akinete-induced cultures carried one to several akinetes during the early stages of differentiation. These young akinetes emitted blue fluorescence that was slightly stronger than that of adjacent vegetative cells (Figure 1B) and was detected as relatively higher 472 nm emission in the acquired spectral data (see Figure 2 below). During their maturation, akinetes continued to accumulate DNA as indicated by increasing intensity of blue fluorescence (Figure 1C). Mature akinetes contained the highest quantities of DNA, but the final amount varied considerably between individual akinetes (Figure 1D). A few akinetes lost their fluorescence properties altogether (indicated by solid arrow in Figure 1D) whereas other akinetes emitted strong red fluorescence (indicated with dashed arrow in Figure 1D3) with minor or no blue fluorescence signal. This observation indicates that akinetes formed a heterogeneous population. The absence of fluorescence may indicate akinetes that lost their viability and their cell content was degraded during the early stages of differentiation. On the other hand, strong red fluorescence was observed in a small fraction of the akinete population. It is postulated that such akinetes had a thicker cell wall that may have formed a barrier against penetration of the Hoechst dye, that otherwise effectively penetrated the majority of akinetes. Such thick-walled akinetes also retained a high chlorophyll fluorescence signal, compared to the majority of akinetes that readily lost their chlorophyll upon fixation with 100% methanol. Akinetes with no fluorescence or with extreme red fluorescence were omitted from further analysis.

Variations in spectral properties along Hoechst-stained *A. ovalisporum* trichomes indicated low level heterogeneity among vegetative cells whereas there were substantial differences between akinetes and their neighboring vegetative cells. Figure 2A shows a short trichome with a terminal akinete at either end. Based on the 472 nm fluorescence emission trace, the akinetes had a higher

DNA content than the vegetative cells along that trichome and most of the DNA was concentrated in the central part of the akinetes. The vegetative cells however, were characterized by intense red fluorescence (655 nm emission line in Figure 2A) and low Hoechst-DNA emission intensity. Spectral properties across Hoechst-stained mature free akinetes indicated high DNA accumulation in the central part of the cell, surrounded by photosynthetic pigment complexes (Figure 2B). The intensity of Hoechst-DNA at its emission maximum (472 nm) varied substantially among akinetes. This high variation is further demonstrated from the high standard deviation associated with the emission spectra of Hoechst-stained akinetes as compared to that of vegetative cells (Figure 3). The frequency distribution of the 472 nm Hoechst-DNA emission intensities in akinetes and vegetative cells further demonstrates the high variability of DNA content in mature akinetes relative to that of vegetative cells (Figure 4). Median intensity values of 70 and 28, and peak width of 34 and 6 for akinetes and vegetative cells respectively, were estimated, suggesting higher DNA content in akinetes relative to vegetative cells.

Genome replication in akinetes

The assumption that the high DNA content in akinetes is organized in multiple identical copies of the cyanobacterial chromosome was verified by determining genome copy number in single akinetes and in cohorts of vegetative cells captured by Laser Micro-Dissection microscopy. Figure 5 shows the efficiency of akinete capture and the empty site after excision and transport, and indicates that the full content of the akinete was catapulted into the collection device. Single akinetes and cohorts of vegetative cells were subjected to qPCR with primer pairs designed to amplify a 170 bp fragment of *16S rRNA*. In the example presented in Figure 5, the *16S rRNA* copy number in three independent single akinete samples varied between 335 and 490, whereas in vegetative cells it ranged between 5 and 14 per cell (54 and 140 copies in a sample of 10 cells). Taking into account the 4 copies of the *rRNA* operon in the *A. ovalisporum* genome, in this example an akinete contained between 84 and 122 genome copies and a vegetative cell contained between 1 and 4 genome copies. This type of experiment was replicated at least 30 times for both akinetes and vegetative cells. Based on the accumulated data we calculated 7.8±3.1 genome copies per vegetative whereas a single akinete contained 119±6 genome copies, 15 times more than a vegetative cell (Table 2). The akinete population showed a broad, close to a normal distribution of genome copies that ranged between 25 and 450 per akinete (Figure 6). The number of genome copies per vegetative cell had a relatively narrow distribution (Figure 6). Results of *16S rRNA* amplification experiments corresponded with those for *ntcA* (Table 2).

Ribosome accumulation

Quantification of ribosome pools in akinetes and vegetative cells was carried out by fluorescence *in situ* hybridization using a universal EUB338 *16S rRNA* probe (Amann et al 1990) conjugated to an Alexa 488 fluorophore. Examples of spectral data are presented in Figure 7. Emission spectra were recorded for individual cells, whether akinete or vegetative, always using the same image area (5 pixels) for data acquisition. Vegetative cells were evenly labeled and their emission spectra (peak at 520 nm) were typical for Alexa 488. Probe hybridization to akinetes, however, varied strongly among cells (Figure 7-A1) with higher average peak intensity than observed in vegetative cells. The spectral data acquired on akinetes and vegetative cells were used to determine the frequency distribution of the Alexa 488 fluorescence intensities (Figure 7B). Median intensity values of 155 and 205 were calculated for vegetative cells and akinetes, respectively.

Nucleic acids accumulate at the expense of inorganic Poly-P

DAPI staining revealed nucleic acid enriched akinetes (blue color) and the presence of Poly-P granules/bodies (yellow-greenish color), of different sizes and shapes, in vegetative cells of *Aphanizomenon* (Figure 8). The absence of Poly-P bodies in mature akinetes was further confirmed by Neisser staining. Spherically shaped Poly-P bodies (dark granules of variable sizes) were abundant in vegetative cells, rarely found in developed akinetes and undetected in mature akinetes (Figure 8).

Discussion

Accumulation of nucleic acids in akinetes of Nostocales (cyanobacteria) has been reported for numerous species and was interpreted as a requirement for dormancy and germination (Kaplan-Levy et al 2010). We applied Hoechst 33258 as specific DNA binding dye to demonstrate high Hoechst-DNA fluorescence signals in akinetes relative to vegetative cells using a single cell spectral analysis approach. However, the precise quantification of the cellular DNA content is rather complicated due to the intricacy of the fluorescence signal originated from a spherical body (either an akinete or a cell) and potential internal cellular quenching of the fluorescence signal. Therefore we used a direct and quantitative, single-cell approach, to show that extensive genome replication accounts for the large nucleic acid pool in akinetes.

We have demonstrated that vegetative cells of *A. ovalisporum* are polyploid, with an average genome copy number of 8, similar to that reported for *Synechococcus* PCC 6301 which ranged between 3 and 18 (Binder and Chisholm 1990) or *Synechocystis* PCC 6803 (Labarre et al 1989).

Polyploidy was also reported for eubacteria such as *Thermus thermophilus* (4-5 genome copies) (Ohtani et al 2010) and for the halophilic archaeon *Halobacterium volcanii* with ~18 genome copies per cell, a number which was down-regulation to 10 genome copies per cell when *H. volcanii* entered stationary phase (Breuert et al 2006). Here we report that the chromosomal content of akinetes in the cyanobacterium *A. ovalisporum* may accumulate to a maximum of 450 copies. With an average value of 119 copies per akinete this is a 15 fold higher than in vegetative cells. Such extreme levels of polyploidy are rare in prokaryotes with a single, disputed, description of polyploidy in the large bacterium *Epulopiscium* (Robinow and Angert 1998, Bresler et al 1998). PCR quantification of the *Epulopiscium* sp. type B genome suggested that this bacterium is highly polyploid with an individual cell containing >10,000 copies of its genome (Mendell et al 2008, Bresler and Fishelson 2003, Liu 2009). If cyanobacterial akinetes represent starvation or aging responses, similar to those that induce stationary phase, we would expect akinetes to show a decrease in polyploidy like that reported for *H. volcanii* (Breuert et al 2006). However, considering the role of akinetes in the cyanobacterial life cycle and its resilience under harsh conditions, high polyploidy may confer a strategic advantage similar to that described for *Deinococcus radiodurans* (Daly and Minton 1995) exposed to high levels of radiation or for *T. thermophilus* at high temperatures. Polyploidy of *A. ovalisporum* akinetes may guarantee the preservation of the integrity of the chromosome and its content over long spells of inactivity. In addition and possibly more importantly, immediate resumption of growth upon akinete germination may be essential to rapidly establish significant populations that gain competitive advantage in the newly established environmental conditions. Processes like DNA replication require significant resources and existing cellular reserves will help to rapidly bridge the gestation period and accelerate cell division during this stage. We also report on high variation in polyploidy within the akinete population which is much higher than the variation between vegetative cells. The source for such a variation could stem from different metabolic status of the differentiating vegetative cell. Such variation may be predicted to affect the dormancy period and the germination efficiency.

In addition to the very substantial polyploidy of akinetes, we show that ribosomes accumulate in akinetes to a higher level than in vegetative cells. The evidence is based on fluorescence *in situ* hybridization with a probe targeting 16S ribosomal RNA and its detection with confocal laser scanning microscopy. While this method cannot be considered strictly quantitative, it provides estimates of the relative ribosome content of cells hybridized and imaged simultaneously and using identical conditions. Assuming that the recorded FISH signal represents mainly 16S rRNA associated with ribosomes, and based on the fact that fluorescence signals were always acquired

from the same area (5 pixels) we estimate that the rRNA density (ribosome number per pixel) in akinetes is approximately 32% higher than in vegetative cells. As a first approximation and due to the larger diameter of akinetes (12 μm versus 6 μm in vegetative cells) we estimate that volumetric ribosome content of akinetes exceeds that of vegetative cells by a factor of 10 (8 fold difference in volume and 1.3 fold in areal density). These estimates should be further verified by direct measurements of single cells as we did to determine polyploidy in akinetes. Nevertheless, our results clearly suggest that accumulation of ribosomes in akinetes is an inherent property of these dormant cells.

Variation in ribosome content in prokaryotes has been correlated to growth conditions and physiological status of the cells. Direct measurements reported that ribosome content in exponentially growing *E. coli* varied between 6,800 and 72,000 copies per cell (Bremer and Dennis 1996, Vandeville et al 2011). Furthermore, the ribosome pool changed significantly with a circa 20-fold increase between the lag and logarithmic growth phase and a drop to less than 1% of maximum after one day of starvation (Nilsson et al 1997). Several *Synechococcus* and *Prochlorococcus* strains showed relatively little change in $rRNA \cdot cell^{-1}$ at low growth rates, linear increase at intermediate growth rates, and a plateau and/or decrease at the highest growth rates (Worden and Binder 2003). Since akinetes represent a temporarily non-dividing entity with low levels of metabolic activity it is surprising to find such a high ribosome content. Why akinetes require high ribosome contents while their metabolic activity is substantially reduced during an extended period of dormancy remains an open question. A possible answer lies in the fact that akinete germination and development of the emerging trichome may require rapid *de novo* synthesis of proteins and an immediate resumption of metabolic activity.

Accumulation of ribosomes and multiplication of the genome in akinetes require the recruitment of cellular resources. Here we present evidence that phosphate is provided via the transformation of phosphate from its storage component (inorganic Poly-P bodies) in vegetative cells to enlarged pools of nucleic acids in akinetes. Inorganic polyphosphate, a linear polymer of orthophosphate residues, is an essential energy source and a reservoir for metabolism and growth (Korenberg 1995) and it plays a role in regulation of fruiting body and spore development in *Myxobacteria* and sporulation in *Bacillus* (Shi et al 2004). Based on cellular P content of a single exponentially grown vegetative cell of *A. ovalisporum* (Hadas et al 2002), the stored inorganic Poly-P should be sufficient for a 10-fold increase in the number of genome copies in an akinete relative to the vegetative cell it has differentiated from. This interpretation suggests a unique function to inorganic

poly-P in Nostocales and implies an essential role of phosphate in the differentiation of akinetes which balance between the conservation of a polymer with high-energy phosphate bonds and the yet unrevealed role of high genome copy number and ribosomes in dormant cells. One exception to this pattern is in some Nostocales species where phosphate limitation appeared to be the major trigger for the development of akinetes (Van Dok and Hart 1996, Meeks et al 2002). However, in many other cases phosphorus was required to allow full development of akinetes (Kaplan-Levy et al 2010).

Acknowledgements

This work was carried out at the Bay Paul Center, Marine Biology Laboratory and supported by the Gruss Lipper Foundation research award (AS). This study was part of the Joint German-Israeli-Project (FKZ 02WT0985, WR803) funded by the German Ministry of Research and Technology (BMBF) and Israel Ministry of Science and Technology (MOST). We thank Ms. Katherine Hammar and Mr. Blair Rossetti for their skillful technical help. Special thanks to Mr. Christopher Rieken, Carl Zeiss Microimaging, Inc. for his resourceful advice and help.

References

Amann R, Binder BJ, Olson RJ, Chisholm SW, Devereux R, Stahl DA (1990). Combination of 16S rRNA-targeted oligonucleotide probes with flow cytometry for analyzing mixed microbial populations. Applied and Environmental Microbiology **56**: 1919-1925.

Bacteriologists SoA (1957). *Manual for Microbiological Methods*. McGraw-Hill: New York.

Banker R, Carmeli S, Hadas O, Teltsch B, Porat R, Sukenik A (1997). Identification of cylindrospermopsin in *Aphanizomenon ovalisporum* (Cyanophyceae) isolated from Lake Kinneret, Israel. *Journal of Phycology* **33:** 613-616.

Binder BJ, Chisholm SW (1990). Relationship between DNA cycle and growth rate in Synechococcus sp. strain PCC 6301. J Bacteriol **172**: 2313-2319.

Bremer H, Dennis P (1996). Modulation of cell parameters by growth rate. In: Neidhardt RCI FC, Ingraham JL, Lin ECC, Low KB, Magasanik B, Reznikoff WS *et al* (eds). *Escherichia coli and Salmonella: Cellular and molecular biology*, 2nd edn. ASM press: Washington DC. pp 1553-1569.

Bresler V, Montgomery WL, Fishelson L, Pollak PE (1998). Gigantism in a bacterium, *Epulopiscium fishelsoni*, correlates with complex patterns in arrangement, quantity, and segregation of DNA. *J Bacteriol* **180:** 5601-5611.

Bresler V, Fishelson L (2003). Polyploidy and polyteny in the gigantic eubacterium *Epulopiscium fishelsoni*. *Marine Biology* **143:** 17-21.

Breuert S, Allers T, Spohn G, Soppa J (2006). Regulated polyploidy in halophilic Archaea. *PLoS ONE* **1:** e92.

Carmichael WW, Mahmood NA, Hyde EG (1990). Natural toxins from cyanobacteria (blue-green algae). In: Hall S, Strichartz G (eds). *Marine Toxins: Origin, Structure and Molecular Pharmacology*. American Chemical Society: Washington DC. pp 87-106.

Codd GA, Morrison LF, Metcalf JS (2005). Cyanobacterial toxins: risk management for health protection. *Toxicology and Applied Pharmacology* **203:** 264-272.

Codd GA, Bell, S.G., Kaya, K., Ward, C.J., Beattie, K.A. and Metcalf, J.S. (1999). Cyanobacterial toxins, exposure routes and human health. *European Journal of Phycology* **34:** 405-415.

Daly MJ, Minton KW (1995). Resistance to Radiation. *Science* **270:** 1318-1318.

Dittmann E, Wiegand C (2006). Cyanobacterial toxins – occurrence, biosynthesis and impact on human affairs. *Molecular Nutrition & Food Research* **50:** 7-17.

426 Fay P (1969a). Cell differentiation and pigment composition in *Anabaena cylindrica*. *Arch*
427 *Mikrobiol* **67:** 62-70.

428 Fay P (1969b). Metabolic activities of isolated spores of *Anabaena cylindrica*. *J Exp Bot* **20:** 100-
429 109.

430 Hadas O, Pinkas R, Malinsky-Rushansky N, Shalev-Alon G, Delphine E, Berner T *et al* (2002).
431 Physiological variables determined under laboratory conditions may explain the bloom of
432 *Aphanizomenon ovalisporum* in Lake Kinneret. *Eur J Phycol* **37:** 259-267.

433 Hense I, Beckmann A (2010). The representation of cyanobacteria life cycle processes in aquatic
434 ecosystem models. *Ecological Modelling* **221:** 2330-2338.

435 Hori K, Okamoto Ji, Tanji Y, Unno H (2003). Formation, sedimentation and germination properties
436 of *Anabaena* akinetes. *Biochemical Engineering Journal* **14:** 67-73.

437 Hudnell HK, Ibelings BW, Havens KE (2008). Cyanobacterial toxins: a qualitative meta–analysis
438 of concentrations, dosage and effects in freshwater, estuarine and marine biota. *Cyanobacterial*
439 *Harmful Algal Blooms: State of the Science and Research Needs*. Springer New York. pp 675-732.

440 Kaplan-Levy RN, Hadas O, Summers ML, Rücker J, Sukenik A (2010). Akinetes - dormant cells of
441 cyanobacteria. In: Lubzens E, Cerda J, Clark MS (eds). *Topics in Current Genetics*. Springer.

442 Kapuscinski J (1995). DAPI: a DNA-specific fluorescent probe. *Biotech Histochem* **70:** 220-233.

443 Karlsson-Elfgren I, Rengefors K, Gustafsson S (2004). Factors regulating recruitment from the
444 sediment to the water column in the bloom -forming cyanobacterium *Gleotrichia echinulata.*
445 *Freshwater Biology* **49:** 265-273.

446 Kornberg A. (1995). Inorganic polyphosphate: toward making a forgotten polymer unforgettable.
447 *J. Bacteriol.* **177**:491-6.

448 Labarre J, Chauvat F, Thuriaux P (1989). Insertional mutagenesis by random cloning of antibiotic
449 resistance genes into the genome of the cyanobacterium *Synechocystis* strain PCC 6803. *J.*
450 *Bacteriol.* **171**:3449-57.

451 Liu SV (2009). How many genomes does the giant bacterium really have? *Logical Biology* **9:** 42-
452 43.

453 Meeks JC, Campbell EL, Summers ML, Wong FC (2002). Cellular differentiation in the
454 cyanobacterium *Nostoc punctiforme*. *Arch Microbiol* **178:** 395-403.

Mendell JE, Clements KD, Choat JH, Angert ER (2008). Extreme polyploidy in a large bacterium. *Proceedings of the National Academy of Sciences USA* **105:** 6730-6734.

Nilsson M, Bülow L, Wahlund K-G (1997). Use of flow field-flow fractionation for the rapid quantitation of ribosome and ribosomal subunits in *Escherichia coli* at different protein production conditions. *Biotechnology and Bioengineering* **54:** 461-467.

Ohtani N, Tomita M, Itaya M (2010). An extreme thermophile, *Thermus thermophilus*, is a polyploid bacterium. *Journal of Bacteriology* **192:** 5499-5505.

Porter KJ, Feig YS (1980). DAPI for identifying and counting aquatic microflora. *Limnol Oceanog* **25:** 943-948.

Robinow C, Angert ER (1998). Nucleoids and coated vesicles of *Epulopiscium* spp. *Archives of Microbiology* **170:** 227-235.

Siderius M, Musgrave A, Van Den Ende H, Koerten H, Cambier P, Van Der Meer P (1996). *Chlamydomonas eugametos* (chlorophyta) stores phosphate in polyphosphate bodies together with calcium. *J Phycol* **32:** 402-409.

Simon RD (1977). Macromolecular composition of spores from the filamentous cyanobacterium *Anabaena cylindrica*. *J Bacteriol* **129:** 1154-1155.

Shi X, Rao NN, Kornberg A (2004). Inorganic polyphosphate in *Bacillus cereus*: Motility, biofilm formation, and sporulation. *Proc. Natl Acad. Sci. USA* **101**:17061-5.

Stanier RY, Kunisawa R, Mandel M, Cohen-Bazire G (1971). Purification and properties of unicellular blue-green algae: order Chroococcales. *Bacteriol Rev* **35:** 171-205.

Sukenik A, Beardall J, Hadas O (2007). Photosynthetic characterization of developing and mature akinetes of *Aphanizomenon ovalisporum* (cyanoprokaryota). *Journal Phycology* **43:** 780-788.

Sukenik A, Stojkovic S, Malinsky-Rushansky N, Viner-Motzini Y, Beardall J (2009). Fluorescence approaches reveal variations in cellular composition during formation of akinetes in the cyanobacterium *Aphanizomenon ovalisporum*. *European Journal of Phycology* **44:** 309-317.

van Apeldoorn ME, van Egmond HP, Speijers GJA, Bakker GJI (2007). Toxins of cyanobacteria. *Molecular Nutrition & Food Research* **51:** 7-60.

Van Dok W, Hart BT (1996). Akinete differentiation in *Anabaena circinalis* (Cyanophyta). *Journal of Phycology* **32:** 557-565.

484 Vendeville A, Larivière D, Fourmentin E (2011) An inventory of the bacterial macromolecular
485 components and their spatial organization. *FEMS Microbiology Reviews* **35**:395-414.

486 Worden AZ, Binder BJ (2003). Growth regulation of rRNA content in *Prochlorococcus* and
487 *Synechococcus* (marine cyanobacteria) measured by whole-cell hybridization of rRNA-targeted
488 peptide nucleic acids. *Journal of Phycology* **39:** 527-534.
489
490

Figure legends

Figure 1: DNA localization during akinete differentiation and maturation in *A. ovalisporum*. Exponentially grown culture and akinete-induced culture stained with Hoechst 33258 and recorded by laser scanning confocal microscopy (excited with a 405 nm laser line). A – trichomes from exponentially grown culture. B – Trichomes from an akinete-induced culture carrying akinetes at their earlier developmental stage. C – A trichome from an akinete-induced culture carrying an akinete in its late differentiation. D – an aggregate of free akinetes from akinete-induced culture. The images presented for each sample are: (1) transmitted light image; (2) wavelength color-coded image and (3) a superposition of image 1 and 2. Note that some mature akinetes completely lack fluorescence signals (neither Hoechst fluorescence nor autofluorescence signals were detected – full arrow in image D3), whereas some akinetes emitted strong phycobilisomes red fluorescence (indicated with dotted arrow in image D3). Scale bars = 20 μm.

Figure 2: Lateral distribution of Hoechst-DNA 472 nm fluorescence (blue trace) and phycobilisome autofluorescence at 655 nm (red line) along a short trichome with (A) terminal akinetes and (B) free mature akinetes. Wavelength color-coded image, present the localization of Hoechst emission (blue) and pigment autofluorescence (red), are shown together with the corresponding lateral scans of fluorescence intensity. Samples were excited with a 405 nm laser line.

Figure 3: Averaged emission spectrum for exponentially grown vegetative cells (A) and free akinetes from akinete-induced culture (B) stained with Hoechst 33258 and recorded by a laser scanning confocal microscopy. The average spectrum and the corresponding standard deviation are calculated from spectra acquired from more than 70 free akinetes or vegetative cells of exponentially grown trichomes.

Figure 4: Frequency distribution of the Hoechst-DNA 472 nm emission signal in the measured population of exponentially grown vegetative cells (open squares, solid line) and free akinetes (open circles, dashed line).

Figure : Amplification plots, baseline-corrected normalized fluorescence (**Rn) as a fur**
amplification cycle, for a 170bp *16S rRNA* fragment from a single akinete (lower left panel - each color lines represent an individual akinete) and for cohorts of 10 exponentially grown vegetative cells (lower right panel - each color lines represent a 10 cells group) of *A. ovalisporum*. A

calibration curve based on a known copy number of a pBlueScript plasmid carrying a 650 bp fragment of the *16S rRNA* was run simultaneously and used to calculate gene copy number in each unknown sample (an akinetes or a cohort of 10 vegetative cells). The micrographs show a single akinete, before (A1) and after (A2) its removal by laser microdissection and laser pulse catapulting (LMPC). Panel B shows a short filament of 10 cells before LMPC.

Figure 6: Frequency distribution of genome copy number per cell in vegetative cells (closed circles, solid line) and free akinetes (open circles, dashed line).

Figure 7: Quantification of cellular pools of ribosome in akinetes and vegetative cells by fluorescence *in situ* hybridization and laser scanning confocal microscopy (samples were excited with the 488 nm line of a 25 mW Ar laser). Wavelength color-coded image (A1 & A2) are presented for Akinetes and vegetative cells respectively. (B) Frequency distribution of the Alexa 488 emitted signal intensity at 520 nm in vegetative cells (open squares, solid line) and in free akinetes (open circles, dashed line).

Figure 8: The presence of nucleic acids and inorganic Poly-P bodies in vegetative cells and akinetes of *A. ovalisporum.* DAPI stained samples of exponentially grown trichomes (A) and a trichome with an akinete from a 2-week-old akinete-induced culture (B), show blue fluorescence of nucleic acids and greenish fluorescence of Poly-P bodies. Neisser stained samples of exponentially grown trichomes (C) and an aggregate of mature akinetes (D) indicate the absence of Poly-P bodies (dark color granules) in mature akinetes. Scale bars =10 μm.

549 **Tables**
550

551 Table 1: A list of primer pairs and oligonucleotide probes used in this study.

552

553

Target	Name	Sequence	Tm ºC
16s rRNA	16sin3	ATTGGGCGTAAAGGGTCTG	60.2
	16srt3	TTCACCGCTACACCAGGAAT	60.4
ntcA	APHntcaF	AAATGCTTGCTCCACCTGTT	59
	APHntcaR	CAGGGTATACGAGGCAGGAG	59
16s rRNA	EUB338	GCTGCCTCCCGTAGGAGT	

554

555 Table 2: Genome copy number in exponentially grown vegetative cells and in free akinetes of *A.*
556 *ovalisporum*. Numbers are average ± standard deviation for large number of independent
557 measurements (in parentheses). The data is based on quantitative amplification of the*16S rRNA*
558 gene and verified by amplification of *ntcA* (for akinetes only).

559

560
561
562

Cell type	Genome copy No.
Exponentially grown vegetative cells (16S)	7.8±3.1 (40)
Free Akinete (16S)	119±62 (48)
Free Akinete (*ntcA*)	100±92 (6)

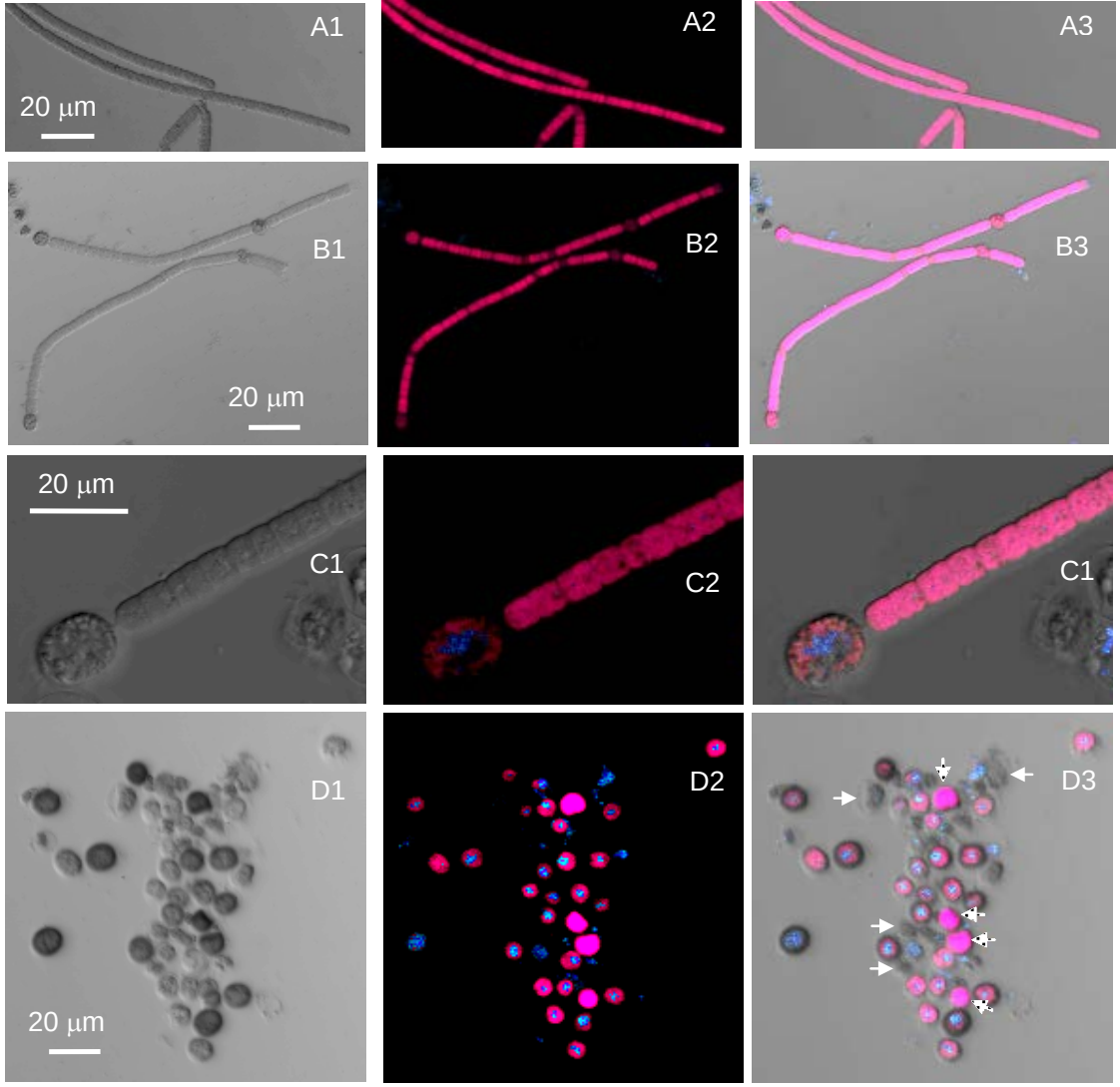

Figure 1: DNA localization during akinete differentiation and maturation in A. ovalisporum. Exponentially grown culture (A) and akinete-induced culture (B to D) stained with Hoechst 33258 prior to their observation and record by laser scanning confocal microscopy. A – trichomes from exponentially grown culture. B – Trichomes from an akinete-induced culture carrying akinetes at their earlier developmental stage; C – A trichomes from an akinete-induced culture carrying an akinete in its late differentiation; D – an aggregate of free akinetes from akinete-induced culture. The images presented for each sample are: light transmission image (1); wavelength color-coded image (2) and a calculated image based on the addition of image 1 and 2 (3). Note that some mature akinetes completely lack fluorescence signals (neither Hoechst fluorescence nor autofluorescence signals were detected – full arrow in image D3), whereas some akinetes emitted strong phycobilisomes red fluorescence (indicated with dotted arrow in image D3) . Horizontal bars indicate a scale of 20 μm.

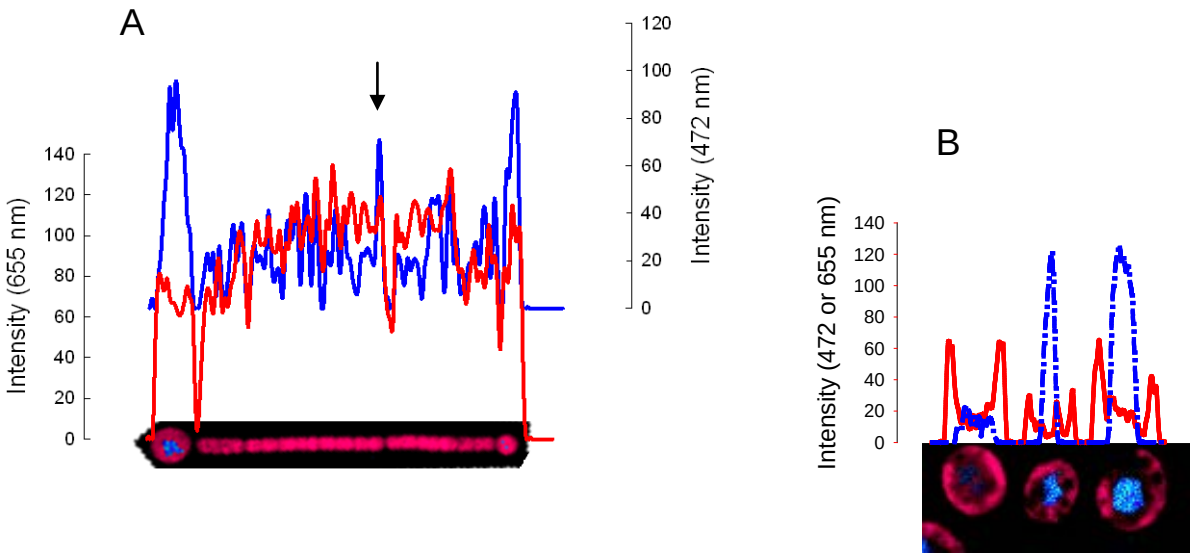

Figure 2: Lateral distribution of Hoechst-DNA 472 nm fluorescence (blue trace) and phycobilisome pigment autofluorescence at 655 nm (red line) along a short trichome with terminal akinetes (A) and free mature akinetes (B). False color images Hoechst emission (blue) and pigment autofluorescence (red) localization are presented together with the corresponding lateral scans of fluorescence intensity. Note the example of a vegetative cell with a slightly higher Hoechst-DNA fluorescence signal (arrow).

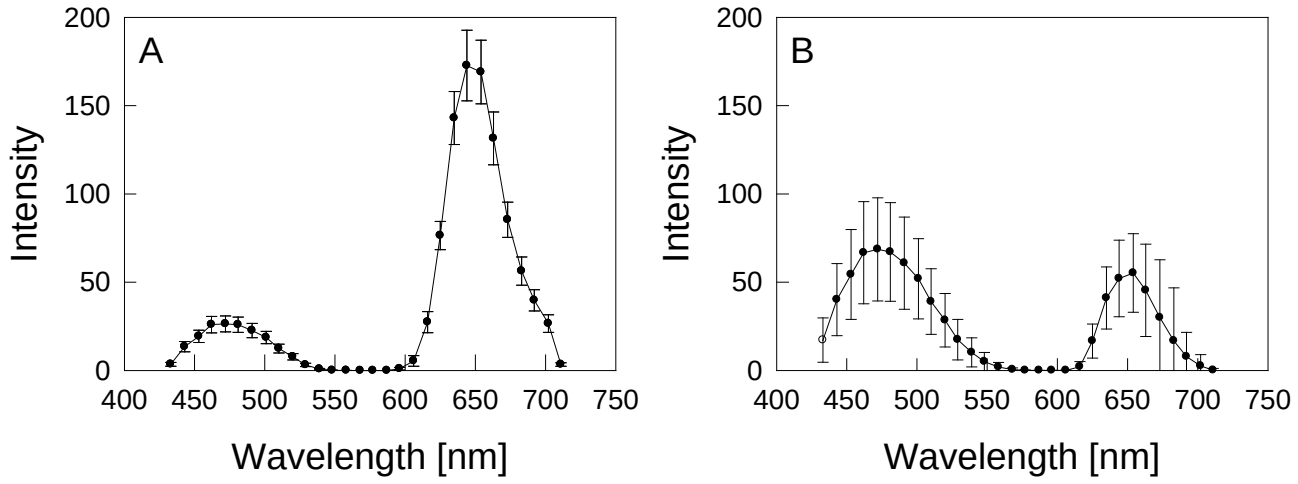

Figure 3: Averaged emission spectrum for exponentially grown vegetative cells (A) and free akinetes from akinete-induced culture (B). The Average spectrum and the corresponding standard deviation calculated from spectra acquired from more then 70 free akinetes or vegetative cells of exponentially grown trichomes.

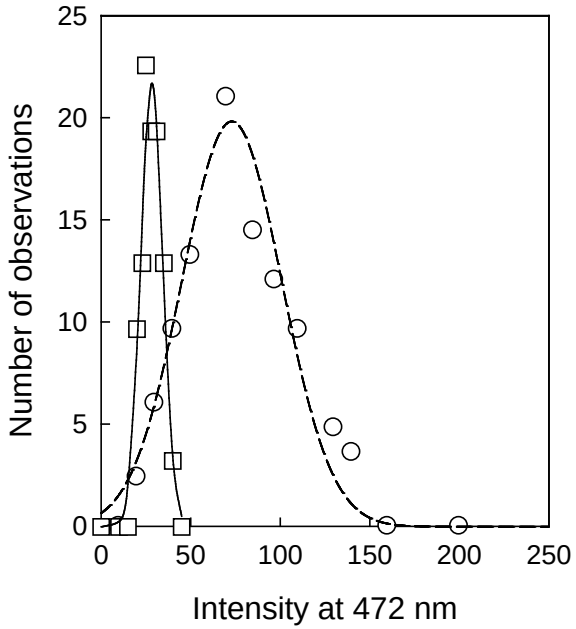

Figure 4: Frequency distribution of the Hoechst-DNA 472 nm emission signal in the measured population of exponentially grown vegetative cells (open squares full line) and free akinetes (open circles dashed line).

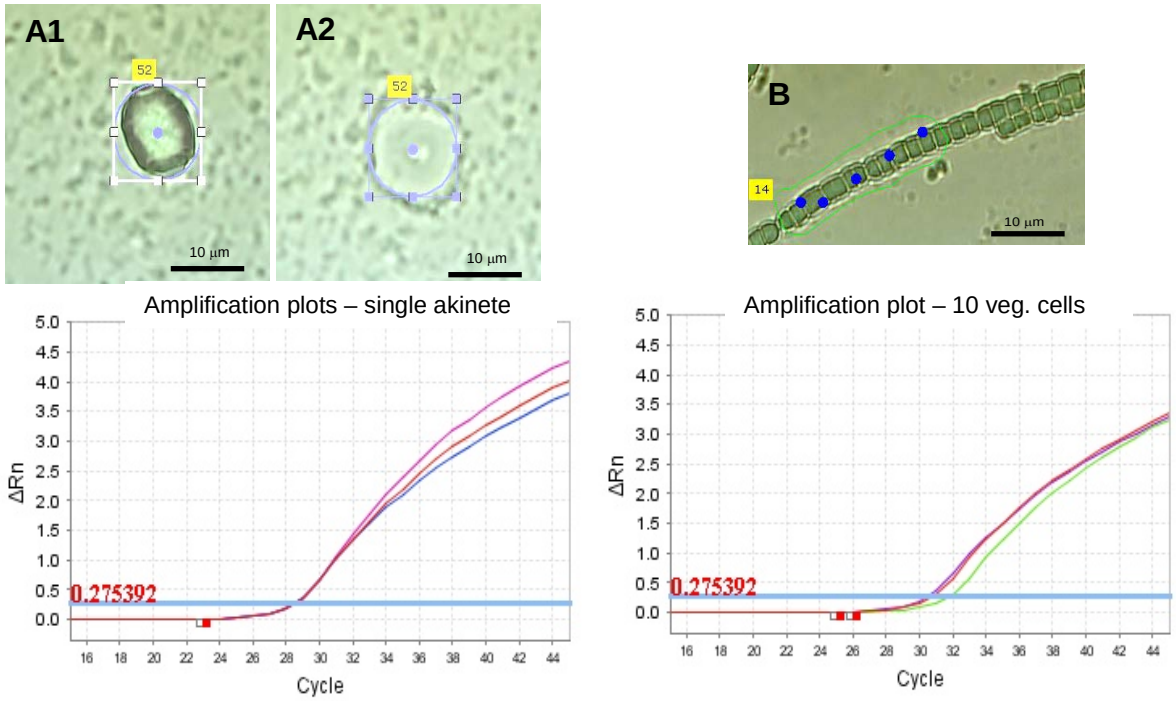

Figure 5: Amplification plots (triplicates) for a 170bp 16S rRNA fragment from a single akinete (A) and from cohorts of 10 exponentially grown vegetative cells (B) of A. ovalisporum. A calibration curve based on a known copy number of a pBlueScript plasmid carrying a 650 bp fragment of the 16S rRNA was run simultaneously. The micrographs show a single akinete, before (left) and after (right) its removal by LMD. Panel B shows a short filament of 10 cells before LMD. The collected samples were immediately submitted to qPCR for determination of the 16S rRNA copy number.

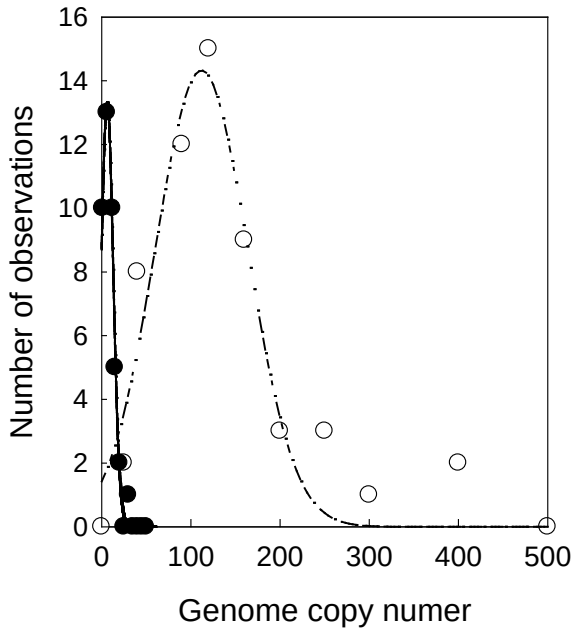

Figure 6: Frequency distribution of genome copy number per cell in vegetative cells (closed circles, solid line) and free akinetes (open circles, dashed line).

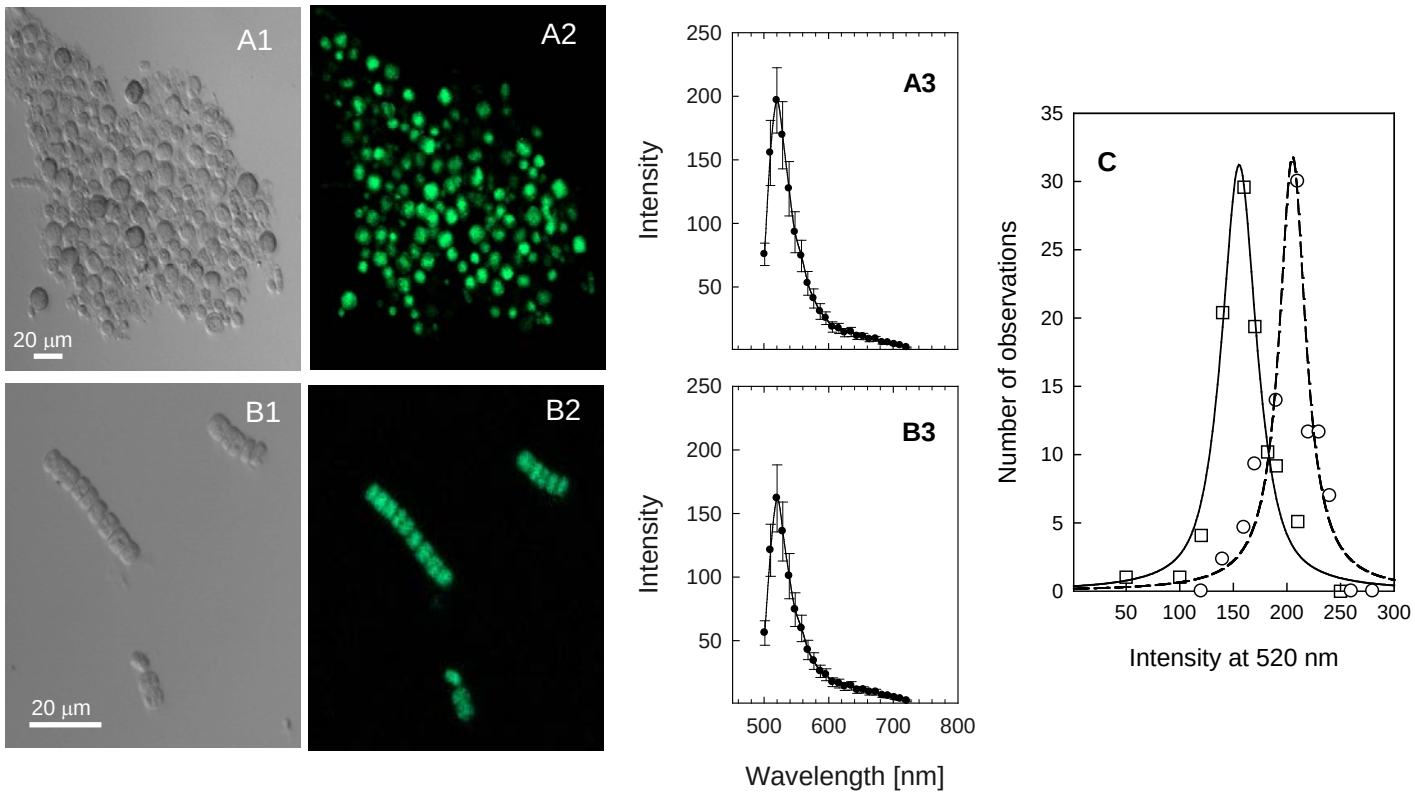

Figure 7: Quantification of cellular pools of ribosome in akinetes (A) and vegetative cells (B) by fluorescence in situ hybridization and laser scanning confocal microscopy. Light transmission image (1) and false color image (2) are presented for each cell type together with averaged emission spectra (3) and frequency distribution of the Alexa 488 emission at 520 nm (C) in vegetative cells (open squares, solid line) and in free akinetes (open circles, dashed line).

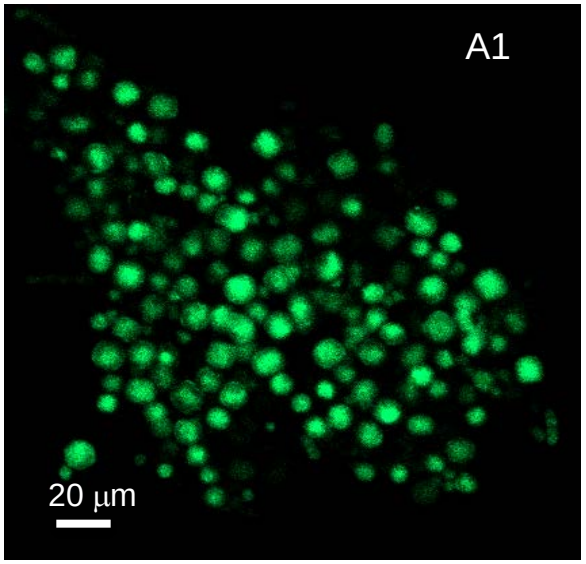
A1
20 μm

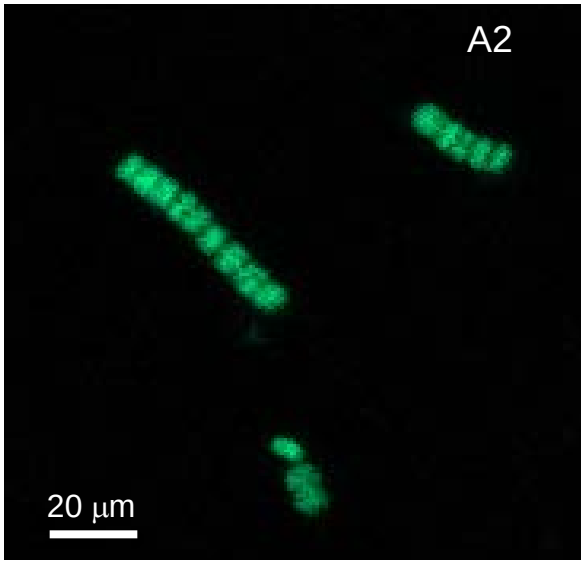
A2
20 μm

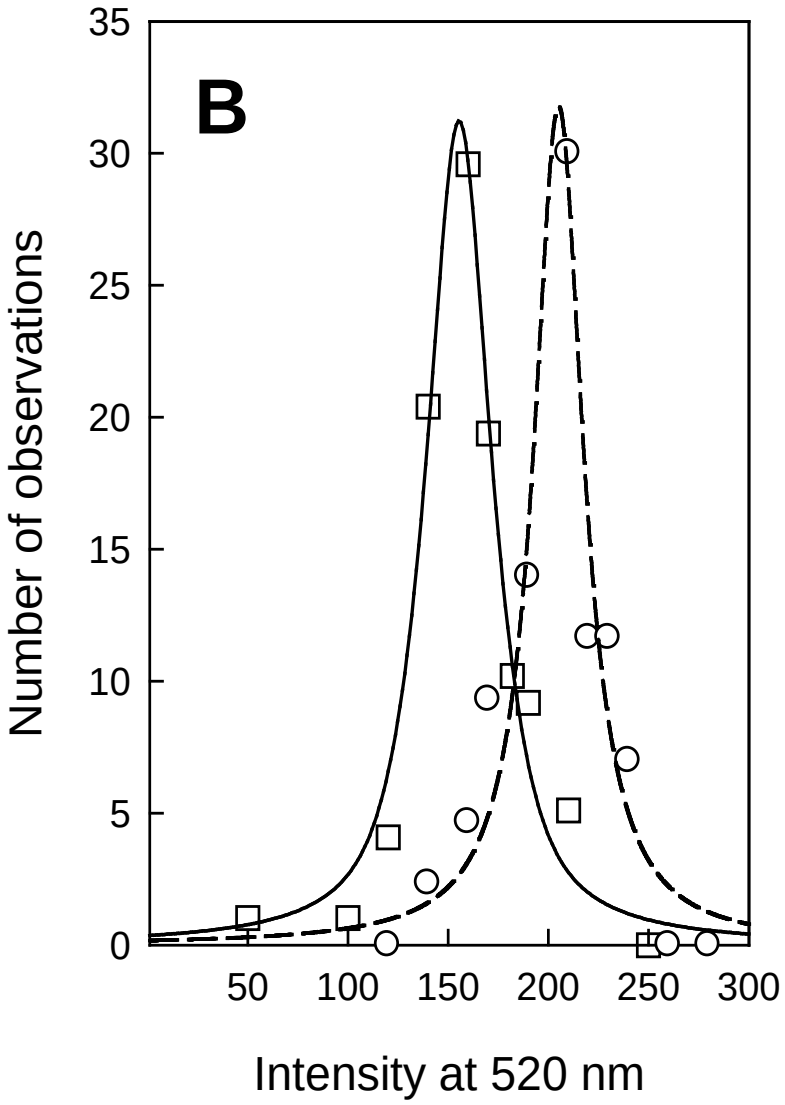
B
Number of observations
Intensity at 520 nm
0
5
10
15
20
25
30
35
50
100
150
200
250
300

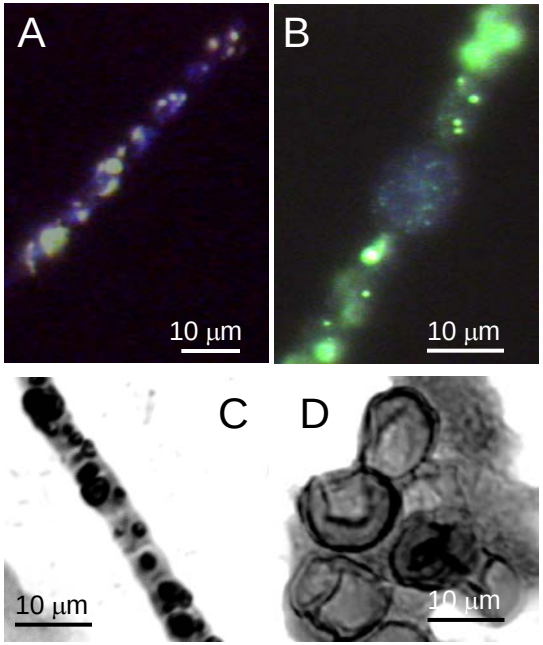

Figure 8: The presence of nucleic acids and inorganic Poly-P bodies in vegetative cells and akinetes of A. ovalisporum. DAPI stained samples of exponentially grown trichomes (A) and a trichome with an akinete from a 2-week-old akinete-induced culture (B), show blue fluorescence of nucleic acids and greenish fluorescence of Poly-P bodies. Neisser stained samples of exponentially grown trichomes (C) and an aggregate of mature akinetes (D) indicate the absence of Poly-P bodies (dark color granules) in mature akinetes. Scale bars =10 μm.